Modelling learning in C. elegans chemosensory and locomotive circuitry for T-maze navigation

Bennet G. Sakelaris[1], Zongyu Li[2], Jiawei Sun[2], Shurjo Banerjee[2], Victoria Booth[1,3], Eleni Gourgou[4,5,*]

[1]Department of Mathematics, [2]Department of Electrical Engineering and Computer Science, [3]Department of Anesthesiology, [4]Department of Mechanical Engineering, [5]Institute of Gerontology, Medical School; University of Michigan, Ann Arbor

*: corresponding author

Short title: Mathematical model of C. elegans T-maze learning

Abstract

Recently, a new type of C. elegans associative learning was reported, where nematodes learn to reach a target arm in an empty T-maze, after they have successfully located reward (food) in the same side arm of a similar, baited, training maze. Here we present a simplified mathematical model of C. elegans chemosensory and locomotive circuitry that replicates C. elegans navigation in a T-maze and predicts the underlying mechanisms generating maze learning. Based on known neural circuitry, the model circuit responds to food-released chemical cues by modulating motor neuron activity that drives simulated locomotion. We show that, through modulation of interneuron activity, such a circuit can mediate maze learning by acquiring a turning bias, even after a single training session. Simulated nematode maze navigation during training conditions in food-baited mazes and during testing conditions in empty mazes is validated by comparing simulated behavior to new experimental video data, extracted through the implementation of a custom-made maze tracking algorithm. Our work provides a mathematical framework for investigating the neural mechanisms underlying this novel learning behavior in C. elegans. Model results predict neuronal components involved in maze and spatial learning and identify target neurons and potential neural mechanisms for future experimental investigations into this learning behavior.

Keywords: C. elegans, learning, locomotion, neuronal circuit dynamics, maze navigation, mathematical model

Word Count: 11360

Introduction

The nematode C. elegans is broadly used to address key neurobiology questions [1]. Despite having only 302 neurons (hermaphrodites), C. elegans are capable of non-associative [2,3] and associative learning [2,4], mainly in the context of chemical cues. Moreover, with their nervous system mapped [5-7] and many of the neuronal connections characterized [8,9], C. elegans have been successfully used to dissect decision making neuronal circuits [10-13].

Lately, mathematical models have been employed to describe and capture neuronal dynamics [11,13-16] in several C. elegans behavior studies, in a way complementary to experimental efforts. In many cases, mathematical modelling is the main means applied to untangle complex neuronal interactions, feeding strategies or locomotion dynamics [17-22]. Interestingly, although learning in C. elegans has been well established and extensively characterized, there are few studies that take advantage of mathematical modelling in their effort to understand the underlying mechanisms [23,24]. Most of these studies focus either on non-associative learning, i.e. habituation [23] or on improved chemotaxis [24], often without taking into account the biological structure of the governing neuronal circuits. However, mathematical models of neuronal circuits have been recruited to explore learning in other systems [25,26] or as stand-alone computational work [27].

Recently, our group [28] characterized a new type of learning in C. elegans, using a custom-made T-maze platform. In this new behavior, young adult C. elegans learn to reach a target arm in an empty maze, after successfully locating reward (food) in a similar training maze (Fig. 1). More specifically, C. elegans nematodes are initially challenged with locating food (E. coli OP50), placed at the end of one maze arm (left side arm in Fig. 1B schematic). Almost 79% of scored worms locate food successfully. When these nematodes are placed in a second, empty T-maze, ~75% of scored nematodes reach the same side maze arm, even though no reward is present. It was shown [28] that functional chemosensation plays a leading role in this food-triggered form of associative learning,

and that other sensory modalities, e.g., mechanosensation and proprioception, are also involved. In addition, it was suggested that C. elegans are likely to use a mixed learning strategy by utilizing both the structural features of the maze and proprioceptive cues. The exact mechanism and neuronal circuits that steer this behavior have not been identified.

Here we present a mathematical model of a simplified C. elegans chemosensory and locomotor neuronal circuitry, activated by the food-released chemical cues, that drives locomotion in a food-baited training maze. We show that, under certain assumptions, such a circuit can produce the learned behavior, as a result of an induced turning bias, even after a single training session. We rely on experimental results reported by Gourgou and colleagues [28], and we verify the realistic nature of simulated worm behavior using new experimental video data, extracted through the implementation of a new, custom-made tracking algorithm, especially developed for the maze environment. Our work provides a mathematical framework for investigating the neural mechanisms underlying this novel learning behavior in C. elegans. Model results replicate key traits of nematode behavior inside the maze, such as percentage of nematodes that locate the bait, percentage of nematodes that learn, their exploratory behavior, and the paths followed during maze navigation. Additionally, model results predict neuronal components involved in maze learning, specifically interneurons that monitor and code for path curvature based on proprioception. Lastly, the model serves as a guide for future experimental work by identifying target neurons and neural mechanisms involved in this learning behavior and provides a foundation for modeling the experimentally observed impact of aging on this behavior.

Methods

Model Development

The main goal of the proposed model is to provide a simplified mathematical framework for the neuronal circuitry that steers C. elegans navigation and learning in a maze environment (Fig. 1) [28].

The model expands upon a previously published and extensively tested C. elegans sensorimotor model [11,29]. For simplicity, we treated the worm as a single point at the head,

with its body following behind. This allows us to examine sensory input at one specific point, for a clear view of the worm's sensorimotor properties.

Each simulated worm was placed in a T-shaped maze inscribed in a 5mm x 5mm square, with functional corridors 1mm wide (Fig 2A). Simulated nematodes use only the functional corridors of the maze.

In building the model, we introduce several assumptions. First, unlike living worms that often climb up the maze walls [28] or even burrow themselves into the agar, model nematodes travel only in two dimensions, crawling on the maze floor without penetrating the wall. This, combined with the absence of indecisive, injured or escaping worms, which occasionally come up in experiments, eliminates censored data.

Second, model nematodes always start the simulation at the bottom of the maze (starting point), oriented in a random direction up the maze corridor (Fig. 2A). This excludes from the simulations much of the exploring behavior that C. elegans might display during the first few seconds in the starting point of the maze, however, does not impact any of the quantitative results.

Third, model worms keep the same ventral/dorsal body orientation with respect to the maze sides during a trip. This assumption is justified by the fact that C. elegans do not flip often [30], unless special conditions apply [31]. For the purposes of this work, we keep the body orientation constant throughout and across the simulations; therefore, the ventral motor neurons always control the body wall muscles that lie toward the left maze side, and the dorsal motor neurons control the ones toward the right maze side. Consequently, nematodes that make a ventral turn or have a ventral turning bias always turn left or counterclockwise, and worms that make a dorsal turn or have a dorsal turning bias always turn right or clockwise.

Lastly, food reward was placed on either the left or the right end of the maze, maintained the same concentration for the entire duration of the simulation, and generated a signal gradient when diffused in the medium (Fig 2B, 2C).

Neuronal Circuit Architecture

Based on the work done by Ghosh and colleagues [11] and the modelling logic adopted by Izquierdo and Lockery [20], we consider a neuronal circuit (Fig. 3) with four main

components: i) the chemosensory neuron AWA, which drives chemotaxis and subsequent food location, ii) the interneuron RIM, which receives input from the AWA and is responsible for steering the worm and controlling the pirouette rate, iii) the motor neurons VMN and DMN which account for all the ventral (V) and dorsal (D) pairs of motor neurons, respectively, and are responsible for locomotion, and iv) the neuronal component Γ, which monitors the worm's instantaneous curvature. AWA, RIM, DMN and VMN correspond to real C. elegans neurons, the role of which has been well established [32,33], whereas Γ accounts for an assumed neuron or collection of neurons.

Due to the undulatory nature of C. elegans locomotion, we can model VMN and DMN as a half-center oscillator [11]. This is achieved through reciprocal inhibition and the implementation of the auxiliary neuronal components IV and ID (Fig. 3). These are not physical neurons that could be found in C. elegans, rather they are implicitly modelled neurons which serve a delayed excitatory connection between VMN and DMN. Similarly, Ω is a component modeled as a neuron, which controls pirouette rate through a probability function (Eq. 13).

Because C. elegans neurons generally produce potentials with graded properties rather than less often observed classic action potentials [34-40], we modeled neurons as leaky integrators [11] with the general equation

$$\tau_m \frac{dV_i}{dt} = -V_i + V_{0,i} + \tanh(I_i) + \xi \qquad \text{(Eq. 1)}$$

where V_i is the (unitless) charge of neuron i, $V_{0,i}$ is the resting potential, I_i is the input, and τ_m is a neuronal time constant. Here, $\tanh$ serves as a sigmoidal function that allows for saturated neuronal signal, observed in C. elegans neurons [41-43]. Finally, ξ is the noise term expressed as a random variable, with mean frequency 0.2 Hz, duration 0.1 seconds and amplitude 0.2.

For the circuit parameters, see also Table S1. Equations 1-14 were solved simultaneously using Runge-Kutta integration with a time step of 0.01s.

Food Gradient

We used a gaussian gradient equation to model the strength of the food signal given by

$$C(x,y) = Ce^{\frac{-r(x,y)^2}{D}} \quad \text{(Eq. 2)}$$

Here C controls the amplitude and D is the diffusion coefficient. Moreover, $r(x,y)$ is the distance between the point (x, y) and the food source (Fig. 2) given by

$$r(x,y) = \begin{cases} \sqrt{(x-x_f)^2 + (y-y_f)^2} & y \geq 4 \\ \sqrt{(x_c-x_f)^2 + (y_c-y_f)^2} + \sqrt{(x-x_c)^2 + (y-y_c)^2} & y < 4 \end{cases} \quad \text{(Eq. 3)}$$

The coordinates (x_f, y_f) and (x_c , y_c) represent the food location and the location of the maze corner nearest to the food, respectively. We use this method to approximate the food gradient rather than simply taking the radial distance, to reflect the assumption that the food-derived chemical cues diffuse more easily through the air-filled corridors of the maze than seeping through the agar-made walls and floor. This is not an exact measurement and may have a small impact on results.

Parameters related to the strength of food gradient are shown in Table S2.

Sensory Neuron

The only sensory neuron in the model is the chemosensory neuron AWA, the dynamics of which is described by the general equation (Eq. 1). Since AWA receives input from the environment rather than other neurons, the input term I_{AWA} is given by the equation

$$I_{AWA} = F - S \quad \text{(Eq. 4)}$$

where F can be considered the fast component of sensory detection and S the slow component [11]. This structure allows the AWA membrane potential to respond transiently to a constant stimulus, which has been observed experimentally[44]. Furthermore, it has been reported that when given a sinusoidal stimulus with the frequency of C. elegans natural head swings, the AWA membrane potential makes oscillations with a similar frequency[44]. This, too, is reflected in the model. Together, these make the AWA sensitive to changes in the food gradient and allows the worms to become accustomed to the scent

of food if the signal is not changing, encouraging the worms to move up the gradient toward the food. We then have

$$\frac{dF}{dt} = \alpha C - \beta F \quad \text{(Eq. 5)}$$

$$\frac{dS}{dt} = \gamma(F - S) \quad \text{(Eq. 6)}$$

where α is the depolarization rate, β is the leak rate, γ is the repolarization rate and finally $C = C(x,y)$ is the strength of the food gradient at coordinates (x, y). Since AWA is sensitive to changes in the food gradient, it is important to understand what the gradient looks like so we can identify which areas are critical for the worm to locate the food (Fig. 2).

For model parameters related to food location (chemotaxis), see also Table S3.

Interneurons and Motor Neurons

For interneuron RIM, motor neurons, and the auxiliary components IV and ID, the I_i term in equation (Eq. 1) is given by

$$I_i = b \sum_{j \in N_i} w_{j \to i} V_j \quad \text{(Eq. 7)}$$

where b is the gain parameter, N_i is the collection of all neurons that send output to i, and $w_{j \to i}$ is the strength of the connection from neuron j to neuron i.

In the absence of sensory input, V_{VMN} and V_{DMN} approach a state of stable oscillations which drive undulations in the worm's locomotion. In order to start these oscillations in the motor circuit, initial conditions for the motor neurons needed to be nonzero. To avoid unnatural movement of the worms in the beginning of the maze, we chose initial conditions on the steady state, setting V_{VMN} to -0.167, V_{DMN} to +0.167, V_{IV} to +0.405, V_{ID} to -0.405.

The Γ Neuron

Γ is a neuronal component modeled as an interneuron, which receives input from the motor circuit. Thus, it tracks the instantaneous geometric curvature of the worm's motion (see Results section and Fig 5) and its activity in the circuit can introduce a turning

bias (see Results section and Fig 6). The bias is achieved by varying the resting potential, $V_{0,\Gamma,}$ according to the equations,

$$V_{0,\Gamma} = m\tanh(\zeta) \quad \text{(Eq. 8)}$$

$$\frac{1}{k}\frac{d\zeta}{dt} = -r\zeta + gV_{\Gamma}V_{AWA} \quad \text{(Eq. 9)}$$

Here, ζ represents the bias term which gets triggered as the worm approaches the food. Activity differences in the AWA and Γ driven by head sweeps across the food gradient cause it to increase when the worm senses a stronger food gradient on its dorsal body side and decreases when it senses stronger food gradient on its ventral body side (Fig. 6, Fig. 8). This means that by the time the worm reaches the food, we would typically expect $V_{0,\Gamma}$ to tend toward either $+m$ or $-m$. Because this is the resting potential of the Γ neuron, $V_{0,\Gamma}$ will be positively or negatively biased as a result.

Simulating Motion

The instantaneous direction of motion changes as a function of the VMN and DMN neurons. This direction is used to calculate the x and y coordinates of the point worm:

$$\frac{d\theta}{dt} = \omega(V_{VMN} - V_{DMN}) \quad \text{(Eq. 10)}$$

$$\frac{dx}{dt} = v\cos(\theta) \quad \text{(Eq. 11)}$$

$$\frac{dy}{dt} = v\sin(\theta) \quad \text{(Eq. 12)}$$

where ω is the undulation amplitude, v is the velocity in mm/s, x and y are in millimeters and θ is in radians. Pirouettes are implemented by changing θ to a random number drawn from a uniform distribution in the interval $[0,2\pi]$. Pirouette frequency in the training maze is given by a probability function depending on the value of V_{Ω}:

$$P(V_{\Omega}) = \begin{cases} 0 & p + w_{\Omega}V_{\Omega} < 0 \\ p + w_{\Omega}V_{\Omega} & 0 \le p + w_{\Omega}V_{\Omega} \le 2p \\ 2p & p + w_{\Omega}V_{\Omega} > 2p \end{cases} \quad \text{(Eq. 13)}$$

Where p is the average pirouette rate of 2.1 pirouettes per minute [11] and w_{Ω} is the unitless proportionality constant equal to 2.1. Because AWA inhibits RIM and RIM excites Ω, V_{AWA} increases when the worm is heading up the food gradient, which causes V_{RIM} and V_{Ω} to decrease. This in turn lowers the probability of a pirouette. Similarly, when the worm is

moving down the gradient, V_{AWA} decreases, which subsequently increases the pirouette rate. The more frequent occurrence of pirouettes when the nematode is moving up the gradient, probably to terminate runs that lead the animal away from the attractant, has been observed experimentally[45].

Additionally, experiments showed that worms spend more time in the control maze than the testing maze[46]. Modeling shows that this result is consistent with trained worms having a lower pirouette rate than naïve worms, so we decreased the value of the pirouette rate parameter, p to be 1.47. This value was chosen to optimize the performance of the model; however, we note that the results of the model are agreeable with experimental results for any value of p between 0.58 and 2.2 pirouettes per minute (Figure S6).

For locomotion-related parameters, see also Table S4.

Learning Connections

During the training phase (Fig. 1B), the Γ neuron only receives input (Fig. 3, black arrows); however, during testing, Γ sends an equal output to VMN and DMN (Fig. 3, red arrows) given by

$$w_{\Gamma \to XMN} = \mathrm{w}\ \mathrm{sgn}(V_{0,\Gamma}) \qquad \text{(Eq. 14)}$$

where $V_{0,\Gamma}$ is the final value determined by equations 8 and 9 at the end of training. This means that $V_{0,\Gamma}$ is positive, then VMN and DMN both receive a positive, oscillating input, which is antiphase to curvature. Similarly, if $V_{0,\Gamma}$ is negative, then VMN and DMN receive a positive, oscillating input which is in phase with curvature. We call the outputs from Γ to VMN/DMN the learning connections.

We justify the plasticity of the above connections as a hypothesized mechanism of learning, since it is has been shown that functionally silent synaptic connections become strengthened when modulatory conditions change [47]. Indeed, neuromodulation can reconfigure circuit properties, and can amend neuronal functions over seconds or minutes[47]. For example, in the modeled circuit, this could be the result of dopaminergic neuromodulation, as C. elegans possesses dopaminergic neurons [48] that are involved in motor behavior control [49], e.g. increased turning behavior [50], that can be affected by

reward-triggered learning [4]. Notably, plasticity of these learning connections would not occur in worms that do not reach the food/reward during training because no reward induced dopamine signaling would have occurred. This is reflected in the model because in this case $sgn(V_{0,\Gamma})$ and thus $w_{\Gamma \to XMN}$ would be equal to zero.

For parameters related to the learning connections, see also Table S5.

Data accessibility statement: All codes related to this work will be made available, upon acceptance of this manuscript, and will be accessible in a public repository (GitHub).
Ethics statement: Experimental animals used in this work were hermaphrodites C. elegans nematode worms, which, as invertebrate animals, do not require IRB approval. In any case, the minimum necessary number of nematodes was used (n=41, as stated in Figure 12).

Maze Tracker

In order to track C. elegans as they traverse a maze, we developed a customized algorithm, the Maze Tracker, that would be effective in the maze environment, and tracks the centroid of the nematode. Standard worm trackers are designed for use with open surface NGM plates, which offer high contrast and low noise, and can track nematodes as they move on 2-dimensional surfaces. In the case of T-mazes [28], most nematodes are moving along three dimensions, the background is non-uniform due to the 3-dimensional maze structure, recordings are often noisy due to camera refocusing, and in some frames the worm in study is momentarily undetectable, moving along wall-floor edges.

To tackle the challenge, the Chan-Vese active contour method [51] is used as a first step to extract contours from the first frame of each recording (Fig. 4A). The user must select the number of iterations for which to run the algorithm as a hyper-parameter. After applying Chan-Vese active contour method, several contours are obtained, so we need to pick the one that is most likely to correspond to the T-maze. This is achieved by finding the contour whose horizontal length and vertical length satisfy the threshold values that are provided by the user. An example of the separated T-maze contour is shown in Fig. 4B.

Next, a T-shape polygon is fitted to the contour. This is required i) to prevent the algorithm from continuing to track an animal after it has escaped the maze and from focusing on a dark non-worm object that lie outside the maze limits. Since the Maze Tracker is based on the difference between frames, an algorithm that shifts its focus between frames would result in errors; ii) due to the top-down imaging system and the light source's perspective, the imaged T-maze border is slightly distorted with respect to the true border – as a result the contour generated by Chan-Vese is often smaller than the real T-maze and must therefore be resized; iii) the generated Chan-Vese contour is not guaranteed to be a perfect T-shape due to noise in the image, however we know that the experimental maze structure was a T-shape by design. Therefore, fitting a T-polygon and assigning it as the area of interest allows the algorithm to track the worm for a larger part of the maze area. Polygon fitting thus allows the use of a consistent T-shape throughout the tracking. This polygon is rotated and shifted to have maximal overlap with the extracted contour.

The problem can be mathematically described as follows:

$$T \approx QP + d1_N^T$$

where T denotes the coordinate matrix of the T-maze contour with size $\mathrm{M} \times \mathrm{N}$, P denotes the generated coordinate matrix of the polygon with size $\mathrm{M} \times \mathrm{N}$, Q is a unitary matrix and d is a displacement vector. The Procrustes Transformation method is applied [52] to solve the problem, which can be written as

$$\hat{Q}, \hat{d} = \underset{Q:\ Q'Q=I,\ d \in F^M}{\arg\min} \|T - (QP + d1_N^T)\|_F$$

Note that F in the subscript denotes the Frobenius norm. An example of the polygon fitting via this transformation can be found in Fig. 4C.

Every frame's rank-1 approximation is computed using singular value decomposition (SVD). To be more precise, suppose a video has L frames, where each frame has size $\mathrm{W} \times \mathrm{H}$, then we build a matrix having size $(\mathrm{WH}) \times \mathrm{L}$. Therefore, an approximation is made, based on all the frames of the video. This approximation can satisfactorily estimate the static background of the maze. Subtracting the approximated background from every frame highlights the motion of the worm, making tracking easier. To track the worm, a diff operation (MATLAB) is performed on every two successive video

frames, where the foreground object, namely a moving worm, can be represented by $I_{i+1}(x,y) - I_i(x,y)$, where I_i denotes the image at the ith frame in a video. The foreground object is calculated for each frame and differences between frames are assumed to account for worm motion (note that this assumption can be considered simplistic as videos are collected in noisy environments, and therefore noise rectification steps are described below). Over the entirety of the video, the tracking result for each frame is concatenated, to generate the final trajectory of the moving worm.

As mentioned earlier, videos collected are often noisy. The most important sources of noise are that i) the experimenter often changes the focus of the camera to more easily track the worm from a human perspective – such a change in focus introduces noise in to the diff operation as successive frames at the point of change can be very different; ii) due to the camera's perspective, it is sometimes hard to see the worm when it is crawling along maze walls. These types of noise usually result in spikes in the detected path (see Fig. 4D, green line).

To rectify this, we solve a binary classification problem to classify every point on a trajectory as "noisy" or "not noisy" based on preceding trajectory points. Our 2-step algorithm utilizes a user-defined threshold and the K-Nearest Neighbor (KNN) algorithm to classify noise points. As a first step, successive points are identified that are further from each other than from the user-defined threshold value, thus noisy points are roughly detected. Next, they are "smoothed" using KNN, as all the points labeled as "not noisy" in the first step are found and the label in the majority of the neighboring points is assigned to the point in question. An outline for the 2-step algorithm is given in the Supplementary Information. The classified result is shown in Fig. 4D.

Currently the Maze Tracker does not track the 3-dimensional motion of the worm, although C. elegans crawl both on the floor and on the walls of the maze (see for example Fig. 4C and [28]). Motion on the maze walls is perceived as 2D motion. This follows the mathematical model, which does not account for C. elegans crawling on the maze walls. Moreover, the Maze Tracker does not allow for quantification of locomotion features, i.e., omega turns, reversals, etc., however neither the experimental nor the model results depend on detailed locomotion events.

Results

We built a model of C. elegans chemosensory and locomotive circuitry, where food-triggered maze learning is achieved through hypothesized learning connections, stemming from reward-evoked neuromodulation. We first present results illustrating the relationship between simulated worms path curvature and activation of neurons involved in the chemotaxis process (training). We then show that, based on the simulated worm's motion in response to food-released chemical cues, plasticity in the modeled circuitry reliably generates a turning bias in the worm's motion, yielding behavioral results consistent with observed behavior of living worms, before (training) and after learning (testing). We demonstrate the reliability of the model, which accounts for different worm trajectories in the maze environment, and we confirm and predict experimental results.

Training Results, Food Location and Learning Acquisition

The modeled neuronal component Γ receives input from the motor circuit and as a result, its activity tracks the instantaneous geometric curvature of the worm's path. In order to test this encoding of curvature, we ran 10,000 simulations of a worm in the Training (food-baited) maze and compared path curvature to V_Γ at every timestep. We found (Fig 5A) that V_Γ was essentially a scalar multiple of curvature by finding a linear fit of $\text{Curvature} = 10.79V_\Gamma$ with $R^2=0.999$, suggesting that the connectivity of the network allows Γ to track curvature very well (see also Supplementary Information).

Next, we explored how *C. elegans'* motion changes in the presence of a food gradient (Figs 5B and 5C). When the model worms do not detect food, the curvature of their paths is symmetric between ventral and dorsal undulations (Fig. 5B); however, upon food detection and the worm's path turning up the food gradient, curvature shifts asymmetrically closer to zero, depending which body side the food is on. For example, when the worm is making a ventral (left) turn as in Figure 5C, the magnitude of curvature is smaller in the negative undulations (blue) than the positive undulations (yellow), as indicated by the color bar.

We then asked whether there was any discernable relationship between the path curvature, the voltage of the chemosensory AWA neuron, and food location (Fig 6). Indeed, there is a strong relationship between the three, especially when the worm first enters the junction of the maze and encounters the food gradient (Fig 6, yellow shaded area in graph, yellow highlighted portion of the worm path). In this part of the maze journey, the AWA voltage makes large oscillations due to the worm moving perpendicularly to the gradient. This means that in each undulation cycle the worm heads up and down the gradient causing the AWA voltage to increase and decrease as well. This is an important part of the trajectory because here the worm first receives information about the location of the food in the maze. In fact, it turns out that the AWA voltage oscillates antiphase with Γ voltage, and thus path curvature, when food is on the left maze side, i.e., on the worm's ventral body side (Fig. 6A) and in phase with Γ voltage and path curvature when food is on the right maze side, i.e., on the worm's dorsal body side (Fig. 6B). This justifies the modeling of ζ (Eq. 9) by showing that it increases when Γ and AWA voltages are in phase and decreases when they are out of phase, providing a method for discriminating the source of the food scent. As a result, when ζ is above zero at the end of training, we expect the food to have been on the right side of the maze, and if it is below zero at the end of training, the food is expected to have been on the left side of the maze.

As a hypothetical mechanism for Γ to dynamically encode curvature properties of the trajectory taken to the food reward, the variable ζ was used to dynamically vary the resting potential, $V_{0,\Gamma,}$ of Γ (see Eq. 8) through the training session. The value of $V_{0,\Gamma}$ reached at the end of the training session reflected whether the food was on the right ($V_{0,\Gamma} > 0$) or left ($V_{0,\Gamma} < 0$) side of the maze (Fig. 7). Indeed, we found that $V_{0,\Gamma}$ could accurately predict the reward location more than 88% of the time (Fig. 7).

As shown in Fig. 7, more than 10% of simulated worms attain biases opposite what we might expect. This can happen when the worms' frame of reference changes so that the food gradient is stronger on its other side. For example, in Fig. 8, Worm 1 takes a path where the peak of the food signal gradient is always on its ventral (left) side, leading to a negative final value of ζ, and in turn of $V_{0,\Gamma}$ (red curve, right). Worm 2, on the other hand, takes an identical path to Worm 1 for the first 63 seconds, but then pirouettes and

crosses the horizontal maze arm so that it becomes oriented with the peak of the food signal gradient now on its dorsal (right) side (blue dashed curve, right). As shown in Fig 6, the largest changes in AWA membrane potential occur when the worm is travelling perpendicularly across the food gradient. This means that between 63 and 75 seconds, $V_{0,\Gamma}$ increases significantly and by the end of training, Worm 2 develops a right (dorsal) bias despite the food originally being on the left (ventral) side of the worm. In fact, the vast majority of the opposite biases acquired in the simulations are attributed to worms moving this way, potentially similar to the living nematode in Example 4, of Fig. 11 and the simulated Worm C of Fig. S8 (see also Suppl. Video SI Video 5).

Testing Results and Learning Expression

After implementing this method of dynamically encoding the location of the reward in relation to the model worm, we investigated how to bias locomotion in a testing maze, absent of a food gradient. A simplified and pronounced example of how to induce a turning bias is presented in Figure 9. In this example, Γ delivers an oscillating input to the motor neurons starting at 20 seconds, for various values of $V_{0,\Gamma}$. This achieves asymmetry in the VMN/DMN-governed undulated path. Depending on whether the input is in-phase or anti-phase with path curvature, the worm will make a dorsal (right) turn or a ventral (left) turn, respectively. In any case, the severity of the turn varies with the mean of the input.

In the neuronal circuit model, we can reliably generate similar inputs to the motor neurons, and thus induce a turning bias, by using $V_{0,\Gamma}$ to bias Γ voltage and by activating the learning connections (Eq 14). Suppose, for example, that the worm finishes the training maze with a positive value for $V_{0,\Gamma}$, signifying that the worm made a dorsal/right turn to find food. Then during locomotion in the testing maze, V_Γ will be oscillating in-phase with path curvature around its positive mean, $V_{0,\Gamma}$. Activation of the learning connections whose input is weighted by $w_{\Gamma \to XMN}$, yields a positive, oscillating input to the motor neurons. As we would expect from Fig. 9B, this causes a dorsal (right side/clockwise) turning bias. Similarly, if the worm finishes the training maze with a negative value for $V_{0,\Gamma}$, then in the testing maze V_Γ will be oscillating in-phase with path curvature around its negative mean, $V_{0,\Gamma}$. However, now $w_{\Gamma \to XMN}$ is negative, so the input of the learning connections to the motor neurons has a positive mean and is making

oscillations antiphase to the worm's path curvature, causing a ventral (left side/counterclockwise) turning bias (Figure 9A). Thus, both the amplitude of change in $V_{0,\Gamma}$ and its sign (positive vs. negative) contribute to encoding the location of the food relative to the worm's position.

Notably, this process accounts for more than just a binary decision of either a ventral or dorsal turning bias, since it generates stronger or weaker biases depending on the value of $V_{0,\Gamma}$. This is highlighted in Fig. 9A, 9B, where different magnitudes of input to motor neurons are presented, oscillating around three different means (warm color lines). As illustrated in the curvature visualization panels of Fig. 9, this results in biases of varying strengths.

Cumulative Results and Model Worms Paths

To quantitatively test the model's ability to replicate maze learning in C. elegans, we simulated 10,000 trials of the maze learning experiment (Fig. 1, and [28]). In each trial, we first simulated a worm in the training maze with food on the left maze end, and if that worm located the food, we activated the learning connections in the model circuit and ran the simulation in the testing maze without the food gradient. The simulated worm learned successfully if the first maze end it reached was the left maze end. We then ran 10,000 trials with food on the right side of the training maze. After running all of the training/testing pairs, we found that model worms located the reward during training (Fig. 10, grey shaded area) and successfully learned the reward location (Fig. 10, green shaded area) at similar percentages as observed experimentally (Fig. 1).

The model allows for an intermediate check of the number of worms that acquired the correct turning bias during training, namely the number of trials in which we would expect the worm to exhibit learning in the testing maze based on the acquired $V_{0,\Gamma}$ bias alone (Fig. 10, non-shaded area). It is hard to compare this to an experimental result, since it is challenging to distinguish between the stages of learning acquisition and learning expression experimentally, however, in most of the simulated worms the model learning mechanism is effectively activated.

We also explored whether the path trajectories of simulated worms were similar to those taken by actual worms in the maze experiments. To that end, we used a custom-built algorithm, the Maze Tracker, to track living nematodes as they traversed T-mazes. As shown in Fig. 11, Column A, C. elegans often explored the starting area of the Training maze before migrating north toward one of the maze ends. Some initial exploration also took place in the Testing maze, but pirouetting occurred less frequently. Although tracking results of Fig. 11A do not account for the total population of worms examined, they are indicative of potential routes followed.

Approximations of the four experimental Training trajectories were then used to train the model (Fig. 11B, Training) and the resulting turning bias was used to seed 100 testing simulations (Fig. 11B, Testing). This led to the model Testing outcome agreeing with the experimental Testing outcome in 78-81% of simulations. Interestingly, the high agreement was even present in example 4 in which the experimental C. elegans exhibited a clockwise bias in the Testing maze and did not reach the correct maze arm. In the Training maze, this worm approached the food area having the food on its right body side (dorsal, for the simulated worm). Since the model suggests that it is the worm's orientation with respect to the food signal, which is learned, as demonstrated in Fig. 8, this leads to the model worm developing a clockwise (dorsal) bias as well. Although this type of path trajectory was not taken by all experimental worms that did not exhibit learning, it is exciting that in this case both the real and the simulated non-learners displayed a similar behavior when approaching the reward. We trained the model on 24 additional experimental trajectories, finding that in total, the model results generally matched experimental testing results in eleven out of fourteen trials where the C. elegans expressed learning and in five out ten trials where the C. elegans did not (Fig. S10). For a detailed description of model worms' paths and biases, see also Fig. S8.

The hypothesis of turning bias acquisition can be further tested experimentally by tracking the locomotion of worms placed on an open surface after training, instead of the testing maze. If a turning bias is acquired, then according to the model, nematodes should be moving with a clockwise or counterclockwise turning bias, even in the absence of a maze structure. If food was on the left arm of the training maze, nematodes would be

expected to receive a counterclockwise bias, while if the food was on the right arm, they would be expected to receive a clockwise bias. Indeed, in a simulation of this experiment, when trained with food on the left maze arm, the model predicts that worms spend 71% of the time moving in a counterclockwise direction, 19% in a clockwise direction, and 10% moving straight. (Fig. 12, green bars).

However, this prediction is expected to be only partially corroborated by experimental data. Although a turning bias may be acquired during training, steering nematodes to follow a clockwise or counterclockwise biased motion, C. elegans interaction with maze walls and floors provides mechanosensation-perceived information important for learning [28]. This is not accounted for in the model. Indeed, when an experiment was performed to test this prediction, living worms spent only 61% of the time moving in a counterclockwise direction when tested on a flat NGM plate, after their maze training (Fig. 12, magenta bars). This is still a significant portion time compared to the portion of time spent moving clockwise (32%) and straight (7%), therefore the model's prediction is indeed partially confirmed, due to the acknowledged exclusion of modeling the structural maze features and the nematodes' interactions with them. This interesting observation showcases the necessity of evaluating modeling results in combination with experimental data. The crosstalk of the two can be highly informative.

Discussion

Foundations of the model

Biology-based neural circuit modelling is a promising and emerging approach that can assist in understanding how the neural circuits process, represent and store information [53]. Favorably, the idea that computational models will contribute to understanding how behavior at the organismal level emerges from the properties of lower level circuits [47] is broadly accepted.

The model proposed here, which is based on biophysical principles, aims to explore a neuronal mechanism that could potentially mediate a recently reported learning behavior [28] in an invertebrate experimental system. In this novel paradigm, young adult C. elegans learn to reach a target maze arm in an empty, testing maze, after successfully locating and tasting reward (food) in a training maze (Fig. 1). The idea is to consider a

simple, minimal circuit that could mediate learning under these conditions. The goal is to create a mathematical framework that will continue to evolve as experimental results keep flowing in. Hence, the two thrusts can be in a constant crosstalk, to eventually identify the neural mechanisms that mediate this maze learning behavior.

The presence of food/reward at one end of the maze (Fig. 2) is what triggers the modeled behavior and activates the neuronal circuit in this study (Fig. 3). In experiments, when C. elegans locate and reach the food, a reward is received. To understand how C. elegans learn from receiving a reward, we considered how they reach the reward in the first place. It is well established that C. elegans approach food using two different forms of chemotaxis: klinotaxis and klinokinesis [20,45], also known as the weathervane [54] and pirouette [55,56] mechanism, respectively. C. elegans only need one of these motion forms for successful chemotaxis; however, they often use a combination of the two to locate food as quickly and efficiently as possible [54].

We considered both motion forms to identify a minimal candidate process for the C. elegans to navigate in the training maze. Therefore, the modeled worms reach food through a combination of klinotaxis and klinokinesis, shifting to more dominant klinotaxis as the worm moves up the attractant gradient. As a result, klinotaxis-like motion continues to be more prevalent throughout testing; however, remnants of klinokinesis are still present with the reduced pirouette rate (Eq. 13, and Results, Simulating Motion section).

The reward-triggered nature of the maze behavior affects the model in multiple ways. It is known that dopamine is important for learning and memory [57,58] and that it is particularly involved in reward-related incentive learning [59]. The role of dopamine in C. elegans nervous system has been well studied [60], and its significance for nematodes' non-associative and associative learning has been established [4,61,62]. Therefore, it is logical to hypothesize that the dopamine pathway is involved in the maze behavior. Indeed, in [28] it was shown that a dop-3 mutant strain, which lacks a dopamine receptor, shows compromised maze performance, although the dopamine-mediated mechanism was not further explored. Similarly, C. elegans reward-triggered improved maze performance was abolished in the dopamine-poor mutant cat-2 [63].

Here, the suggested model takes advantage of the neuromodulatory effect of dopamine, when it assumes the emergence of synaptic signaling from the neural component Γ to the VMN and DMN motor neurons as a result of locating the food (Fig. 3). This is based on the concept that otherwise silent synaptic connections are strengthened under the effect of reward-evoked dopamine. Thus, the ability of the circuit to mediate learning stems from the dopamine-induced plasticity of the Γ component. Indeed, it is well established that neuronal dynamics and neuromodulatory mechanisms reconfigure circuits [64] to make them capable of variable outputs under modulator control [47].

Maze learning experimentally observed in C. elegans resembles spatial working memory [65], due to its short timeframe and sensitivity to distraction [28]. Working memory is attributed to increased dopamine receptor density in the brain [65,66], and increased persistent neuronal activity [66,67]. In addition, enhanced functional connectivity, dopamine release and sensitivity, are of key importance in the overall mechanism of working memory [68]. Therefore, existing literature supports the synaptic facilitation and plasticity assumed in the model as the basis of maze learning.

Importantly, model worms locate the food and learn to reach target maze locations (Fig. 10) at similar percentages as observed experimentally (Fig. 1). The difference between the percentage of model worms that acquired the correct bias and the percentage of worms that expressed learning (Fig. 10) could be attributed to the effect of noise or to pirouette-induced distraction during testing. Interestingly, the comparison between the path trajectories of experimental and simulated worms (Fig. 11) confirms the model's ability to realistically reproduce C. elegans locomotion in the maze environment, both in the presence of food (training) and during testing. This is a welcomed strength, since we did not rely on trajectory-describing metrics to build the model, hence the ability of the model to successfully reproduce C. elegans trajectories came as a result of the circuit's properties.

Limitations of the Model

The modeled circuit includes a chemosensory neuron, interneurons and motor neurons, with the addition of neuronal components that are responsible for locomotion features and enable learning (Fig. 3). Experimental results [28] show that C. elegans performance in the maze is a multisensory behavior and requires the contribution of mechanosensation (for food location and learning), and importantly, of proprioception (for learning). The current modeling effort constitutes the first attempt of a parsimonious model capable of capturing C. elegans maze learning under certain conditions. We opted for a simple circuit, with only external chemosensory input. At the same time, although the model does not assimilate any mechanosensory input, the notion of proprioception is present, without explicitly modeling proprioceptive neurons. To this end, the assumed component Γ, which monitors curvature, could represent a neuron expressing mechanosensitive channels involved in proprioception, e.g. TRPN and TRPC [69]. This way, the function of monitoring motion curvature, which is pivotal in the proposed model (Figs. 5 and 9), would be tied to monitoring body bending.

C. elegans body orientation while traversing the maze is found not to be of critical importance for learning, but it could still be a contributing factor for some of the experimental results [28]. In the proposed model, ventral/dorsal body orientation was taken into account, and in fact it was important for the model worms to acquire a turning bias (Figs. 6, 7, 8). It is possible that in living worms the contribution of body orientation is replaced with more detailed proprioceptive cues on the body posture and motion, as well as with feedback on the body's interaction with the structural features of the maze [28]. Indeed, experimental data suggests that multiple TRP channels, which are known to mediate proprioception in both mid-body and the head area [70,71], were involved in maze learning [28]. Incorporating multisensory integration is a main goal as we work to update and fine tune the model. At the same time, it is interesting that the suggested model can account for learning with just chemosensory input and targeted key assumptions.

Lastly, simulated worms pirouetted less in general than the actual worms (Fig. 11). It is well established that when a C. elegans encounters an obstacle with its nose tip, it usually backs up and pirouettes [72,73], and the plasticity of the turning behavior has also been reported[22]. Although this was not always the case when C. elegans encountered

the maze walls in the maze experiments [28], as nematodes might start climbing up the wall, they certainly sometimes engaged in similar obstacle avoidance behavior. This behavior is omitted from the model to keep the network minimal. C. elegans' interaction with the maze walls is modeled only coarsely, also because no 3-dimensional locomotion is considered.

Predictions of the Model

Predictions generated by the model are either confirmed by experimental results or they propose a number of experiments that would further elucidate the maze learning mechanism. As a first indication, an almost identical percentage of experimental and simulated worms reach the same maze side in training and testing (Figs 1 and 10), confirming the overall dependability of the model.

Qualitative and quantitative comparisons between living and simulated worms endorse the key model hypothesis of the Γ curvature-monitoring component. Given that C. elegans use a varying combination of klinotaxis/klinokinesis to maximize food location efficiency and rapidity [54], we conclude that the klinotaxis/klinokinesis mix changes during training, and shifts in favor of klinotaxis once the worm orients itself toward the food. Consequently, one could expect that when they learn, nematodes acquire a mainly klinotaxis-based turning bias. This is reflected in the modeled circuitry where in trained worms, Γ causes a weathervane-like clockwise or counterclockwise turning bias; however, as explained above, the model nematodes' motion in the testing maze comes partially as a result of dampened klinokinesis (reduced pirouette rate), which allows the turning bias to take effect.

As a result, the model predicts that locomotion of successfully trained nematodes is different than of naïve worms, in two ways. First, in an empty maze, trained model C. elegans pirouette noticeably less often than untrained ones (see Methods, Simulating Motion). Second, trained model worms' paths consistently present either a clockwise or counterclockwise bias. Indeed, many of the experimental worm paths also show reduced pirouette rate during testing (Fig 11A). The similarities extend also to the turning bias, since in each example of Fig. 11A the worm's path in the testing maze features a strong

curve which is absent in the training maze. This was investigated more thoroughly by analyzing the movement of C. elegans that were allowed to roam on an open surface after being trained in the training maze (Fig 12). It was found that living worms exhibited noticeable turning biases as suggested by the in-silico experiments, providing further support for the model.

The increase in performance can be attributed to two factors. First, worms which were biased toward the food arm tended to develop stronger biases toward the food arm because magnitude of the resting potential of Γ tended to increase. Second, worms which were biased away from the food were less successful in the next training maze, meaning less of them were allowed to move on to the next phase of the experiment. We found that worms which acquired strong biases toward the food arm were able to successfully complete the subsequent training more than 95% of the time (Fig. S9) and almost always retained a strong bias toward the food arm. Worms with weaker biases successfully completed the subsequent training about 85% of the time and developed stronger biases approximately 80% of the time. However, only about 55% of worms which were biased away from the food arm were able to successfully complete the training maze. Altogether this meant that by the end of the fourth round of training, nearly all worms were strongly biased toward the maze arm, implying that C. elegans may be able to learn more effectively with a repeated training protocol.

Furthermore, as explained above, the model hypothesizes a decisive role for reward-mediated plasticity, perhaps through dopamine signaling. The contribution of the dopamine pathway, of neurons expressing dopamine receptors and of dopaminergic neurons in C. elegans spatial maze learning has not been investigated. Several experiments can be conducted to test this prediction, including, but not limited to, genetic ablation or inactivation of targeted neurons, strains with loss-of-function mutations of dopamine receptors components and targeted use of dopamine inhibitors.

Another major model hypothesis is the function of Γ, as a neuronal component that monitors motion curvature and is subject to neuromodulation-driven plasticity. Consequently, a series of experiments can be designed to test targeted candidate

interneurons or command motor neurons. Note that this role could be played by a collection of neurons with feedback connections.

Model extensions

A very exciting property of the proposed mathematical framework is its ability to operate as a platform for modeling efforts of more complex phenomena, like aging. Gourgou and colleagues [28] report maze learning deterioration in middle aged animals. The exact component or operation of the steering neuronal circuitry that is affected by aging remains to be elucidated. However, the finding of aging-driven learning decline in C. elegans corroborates previous work [74,75].

The proposed model offers three sites, namely model parameters, that could potentially be associated with aging-driven learning deterioration (see also Suppl. Information): i) w (Eq. 1 and Table S1), which is the magnitude of the connection between Γ and the ventral and dorsal motor neurons, ii) k (Eq. 9 and Table S5), which controls the sensitivity of the bias term ζ to sensory input, and iii) m (Eq. 8 and Table S5) which is the maximum magnitude of the change in resting potential of Γ as a result of learning.

Reduced magnitude of the connection between Γ and the motor neurons is related to the learning connections (red arrows in Fig. 3). Physiologically, this corresponds to aging-related decreased ability to achieve working memory [76,77] through strengthening synaptic connections. These connections in the model are hypothesized to be the result of dopamine-mediated neuromodulation. Interestingly, the dopamine system is reported to undergo significant age-related decline [78,79].

Reduced sensitivity of the bias to sensory input would mean that the turning bias acquired by Γ, which is then input to VMN/DMN motor neurons, is weaker. This would result from a reduced signal that Γ receives from its upstream neurons, including sensory ones, or from reduced susceptibility of Γ to the input. Therefore, such a change could be justified by aging-related decline in secondary sensory neurons performance, which has been reported to occur in a context-specific manner [80], and has been correlated to impaired neurotransmission production [80].

The third aging-related model target refers to reduced maximum magnitude of the resting potential of Γ as a result of learning. This represents the sensitivity of Γ to the turning bias signal received in the form of input from the motor neurons during training, or the ability of Γ to induce cellular plasticity. The mechanism of bias acquisition is not explicitly modeled here, therefore the exact biological mechanism by which aging could affect it is not clear. However, the suggested modification could be related to reduced neurotransmission [81], age-related alterations in neurotransmitter receptors [82] or aging-related functional decline of ion channels [83,84].

Since aging is a systemic phenomenon, we investigated the effect of all three interventions combined, and the outcome is presented in Fig. 13 and in a web-based interactive figure (http://www-personal.umich.edu/~bennets/aging_figure.html). The modeled circuitry and parameters presented in this work refers to young adults ($w = 0.2$, $m = 0.7$, $k = 1$), and is capable of successful learning as it operates at the yellow/orange area of the surface plot in Fig. 13C. Aging-derived decreases in each of these parameters reduces the percentage of simulated worms that exhibit successful learning in the testing maze. The effect of each individual potentially aging-related parameter (w, k, m) on worm learning is shown in Fig. S5.

It is noted that in the present work aging is not modeled on a biophysical basis. At the same time, we consider it important that the model is constructed in a way that welcomes future extensions and stands capable of integrating physiological mechanisms that could impact the core hypothesis of learning. Lastly, whether maze learning in C. elegans is an adaptive behavior or a side-effect of associative learning remains to be seen. Deciphering the complete neuronal circuitry that steers this behavior may help shed light on this question. We hope that the mathematical framework presented here can contribute to this effort.

Conclusions

Mathematical modeling does not have to act a posteriori to the experimental component of a research effort, but instead can spark experimentation by proposing a priori a justified hypothesis [85]. We aim to enhance this process with the introduction of

this biophysically based mathematical model for chemosensory and locomotive neural circuitry in C. elegans that is capable of reproducing experimentally observed learning behavior in a T-maze. While we have taken a parsimonious modeling approach, a strength of the proposed model is the generation of several experimentally testable hypotheses. These hypotheses refer to the neural mechanisms which generate plasticity in C. elegans' neural circuitry that may be responsible for the observed learning behavior. In addition, our model framework acts as a platform for investigating effects of other phenomena involved in worm maze learning, such as aging.

Acknowledgements

We thank Drew Clayborn for his contribution during initial steps of this effort, Jason Corso and Vikas Dhiman for initial discussions regarding development of Maze Tracker, and Allen Hsu for use of space and equipment. EG is the recipient of NIH-NIA award K01-AG057833 (provided support for EG and BGS). The content is solely the responsibility of the authors and does not necessarily represent the official views of the National Institutes of Health. The funders had no role in study design, data collection and analysis, decision to publish, or preparation of the manuscript.

Authors' contributions

BGS built the mathematical model, ran simulations, analyzed data, generated figures, and wrote the manuscript. ZL and JS created the Maze Tracker algorithm, analyzed experimental videos and contributed to manuscript writing. SB assisted with building the Maze Tracker and edited parts of the manuscript. VB provided advice and input on model development, reviewed and edited the manuscript, and helped with supervising research. EG conceived the idea, generated figures, collected videos, analyzed data, wrote and edited manuscript, and supervised research. All authors reviewed and approved the manuscript.

Conflict of interest: The authors state that they have no conflict of interest.

Abbreviations: VMN, ventral motor neuron; DMN, dorsal motor neuron; XMN, ventral or dorsal motor neuron; NGM, nematode growth medium; SVD, singular value decomposition; KNN, k-nearest neighbor; TRP, transient receptor potential; TRPN, transient receptor potential - no mechanoreceptor potential C; TRPC, transient receptor potential - canonical

References

1 Sengupta, P. & Samuel, A. D. T. C. elegans: a model system for systems neuroscience. *Current opinion in neurobiology* **19**, 637-643, doi:10.1016/j.conb.2009.09.009 (2009).

2 Rankin, C. H., Beck, C. D. O. & Chiba, C. M. Caenorhabditis elegans: A new model system for the study of learning and memory. *Behavioural Brain Research* **37**, 89-92, doi:https://doi.org/10.1016/0166-4328(90)90074-O (1990).

3 Rankin, C. H. & Broster, B. S. Factors affecting habituation and recovery from habituation in the nematode Caenorhabditis elegans. *Behav Neurosci* **106**, 239-249 (1992).

4 Ardiel, E. L. & Rankin, C. H. An elegant mind: learning and memory in Caenorhabditis elegans. *Learn Mem* **17**, 191-201, doi:10.1101/lm.960510 (2010).

5 White, J. G., Southgate, E., Thomson, J. N. & Brenner, S. The Structure of the Nervous System of the Nematode Caenorhabditis elegans. *Philosophical Transactions of the Royal Society of London. B, Biological Sciences* **314**, 1-340, doi:10.1098/rstb.1986.0056 (1986).

6 Varshney, L. R., Chen, B. L., Paniagua, E., Hall, D. H. & Chklovskii, D. B. Structural properties of the Caenorhabditis elegans neuronal network. *PLoS Comput Biol* **7**, e1001066, doi:10.1371/journal.pcbi.1001066 (2011).

7 Cook, S. J. *et al.* Whole-animal connectomes of both Caenorhabditis elegans sexes. *Nature* **571**, 63-71, doi:10.1038/s41586-019-1352-7 (2019).

8 Towlson, E. K., Vértes, P. E., Ahnert, S. E., Schafer, W. R. & Bullmore, E. T. The Rich Club of the C. elegans Neuronal Connectome. *The Journal of Neuroscience* **33**, 6380-6387, doi:10.1523/JNEUROSCI.3784-12.2013 (2013).

9 Arnatkeviciute, A., Fulcher, B. D., Pocock, R. & Fornito, A. Hub connectivity, neuronal diversity, and gene expression in the C. elegans connectome. *bioRxiv*, doi:10.1101/207134 (2017).

10 Faumont, S., Lindsay, T. H. & Lockery, S. R. Neuronal microcircuits for decision making in C. elegans. *Curr Opin Neurobiol* **22**, 580-591, doi:10.1016/j.conb.2012.05.005 (2012).

11 Ghosh, D. D., Sanders, T., Hong, S., McCurdy, L. Y., Chase, D. L., Cohen, N., Koelle, M. R., Nitabach, M. N. Neural Architecture of Hunger-Dependent Multisensory Decision Making in C. elegans. *Neuron* **92**, 1049-1062, doi:10.1016/j.neuron.2016.10.030 (2016).

12 Jarrell, T. A. *et al.* The connectome of a decision-making neural network. *Science* **337**, 437-444, doi:10.1126/science.1221762 (2012).

13 Tanimoto, Y. *et al.* Calcium dynamics regulating the timing of decision-making in C. elegans. *eLife* **6**, e21629, doi:10.7554/eLife.21629 (2017).

14 Scholz, M., Dinner, A. R., Levine, E. & Biron, D. Stochastic feeding dynamics arise from the need for information and energy. *Proceedings of the National Academy of Sciences* **114**, 9261-9266, doi:10.1073/pnas.1703958114 (2017).

15 Roberts, W. M. *et al.* A stochastic neuronal model predicts random search behaviors at multiple spatial scales in C. elegans. *Elife* **5**, doi:10.7554/eLife.12572 (2016).

16 Kato, S., Xu, Y., Cho, C. E., Abbott, L. F. & Bargmann, C. I. Temporal responses of C. elegans chemosensory neurons are preserved in behavioral dynamics. *Neuron* **81**, 616-628, doi:10.1016/j.neuron.2013.11.020 (2014).

17 Mirzakhalili, E., Epureanu, B. I. & Gourgou, E. A mathematical and computational model of the calcium dynamics in Caenorhabditis elegans ASH sensory neuron. *PLOS ONE* **13**, e0201302, doi:10.1371/journal.pone.0201302 (2018).

18 Soh, Z., Sakamoto, K., Suzuki, M., Iino, Y. & Tsuji, T. A computational model of internal representations of chemical gradients in environments for chemotaxis of Caenorhabditis elegans. *Scientific Reports* **8**, 17190, doi:10.1038/s41598-018-35157-1 (2018).

19 Izquierdo, E. J. & Beer, R. D. The whole worm: brain-body-environment models of C. elegans. *Curr Opin Neurobiol* **40**, 23-30, doi:10.1016/j.conb.2016.06.005 (2016).

20 Izquierdo, E. J. & Lockery, S. R. Evolution and Analysis of Minimal Neural Circuits for Klinotaxis in Caenorhabditis elegans. *The Journal of neuroscience : the official journal of the Society for Neuroscience* **30**, 12908-12917, doi:10.1523/JNEUROSCI.2606-10.2010 (2010).

21 Klein, M. *et al.* Exploratory search during directed navigation in C. elegans and Drosophila larva. *eLife* **6**, e30503, doi:10.7554/eLife.30503 (2017).

22 Calhoun, A. J., Chalasani, S. H. & Sharpee, T. O. Maximally informative foraging by Caenorhabditis elegans. *eLife* **3**, e04220, doi:10.7554/eLife.04220 (2014).

23 Hasani R. M., F. M., Beneder V. , Grosu R. Non-Associative Learning Representation in the Nervous System of the Nematode Caenorhabditis elegans. *arXiv* **e-print 1703.06264** (2017).

24 Demin, A. V. & Vityaev, E. E. Learning in a virtual model of the C. elegans nematode for locomotion and chemotaxis. *Biologically Inspired Cognitive Architectures* **7**, 9-14, doi:https://doi.org/10.1016/j.bica.2013.11.005 (2014).

25 Wei, H., Dai, D. & Bu, Y. A plausible neural circuit for decision making and its formation based on reinforcement learning. *Cogn Neurodyn* **11**, 259-281, doi:10.1007/s11571-017-9426-4 (2017).

26 Garst-Orozco, J., Babadi, B. & Ölveczky, B. P. A neural circuit mechanism for regulating vocal variability during song learning in zebra finches. *eLife* **3**, e03697, doi:10.7554/eLife.03697 (2014).

27 Maass, W., Joshi, P. & Sontag, E. D. Computational Aspects of Feedback in Neural Circuits. *PLOS Computational Biology* **3**, e165, doi:10.1371/journal.pcbi.0020165 (2007).

28 Gourgou, E., Adiga, K., Goettemoeller, A., Chen, C., Hsu, A-L. Caenorhabditis elegans Learning and Decision-Making in a Structured Environment is a Multisensory Behavior. 57 (2020). http://dx.doi.org/10.2139/ssrn.3701942.

29 Cohen, N. & Sanders, T. Nematode locomotion: dissecting the neuronal-environmental loop. *Curr Opin Neurobiol* **25**, 99-106, doi:10.1016/j.conb.2013.12.003 (2014).

30 Schwarz, J. & Bringmann, H. Analysis of the NK2 homeobox gene ceh-24 reveals sublateral motor neuron control of left-right turning during sleep. *eLife* **6**, e24846, doi:10.7554/eLife.24846 (2017).

31 Singh, R. N. & Sulston, J. E. Some Observations On Moulting in Caenorhabditis Elegans. *Nematologica* **24**, 63-71, doi:doi:https://doi.org/10.1163/187529278X00074 (1978).

32 Bargmann, C. I. Chemosensation in C. elegans. *WormBook : the online review of C. elegans biology*, 1-29, doi:10.1895/wormbook.1.123.1 (2006).

33 Hart, A. C. in *WormBook : the online review of C. elegans biology* (ed V. Ambros) (The C. elegans Research Community, 2006).

34 Geffeney, Shana L. *et al.* DEG/ENaC but Not TRP Channels Are the Major Mechanoelectrical Transduction Channels in a C. elegans Nociceptor. *Neuron* **71**, 845-857, doi:https://doi.org/10.1016/j.neuron.2011.06.038 (2011).

35 Goodman, M. B., Hall, D. H., Avery, L. & Lockery, S. R. Active currents regulate sensitivity and dynamic range in C. elegans neurons. *Neuron* **20**, 763-772 (1998).

36 Lindsay, T. H., Thiele, T. R. & Lockery, S. R. Optogenetic analysis of synaptic transmission in the central nervous system of the nematode Caenorhabditis elegans. *Nat Commun* **2**, 306, doi:10.1038/ncomms1304 (2011).

37 Liu, Q., Hollopeter, G. & Jorgensen, E. M. Graded synaptic transmission at the Caenorhabditis elegans neuromuscular junction. *Proc Natl Acad Sci U S A* **106**, 10823-10828, doi:10.1073/pnas.0903570106 (2009).

38 Liu, P. *et al.* Genetic dissection of ion currents underlying all-or-none action potentials in C. elegans body-wall muscle cells. *The Journal of Physiology* **589**, 101-117, doi:10.1113/jphysiol.2010.200683 (2011).

39 Mellem, J. E., Brockie, P. J., Madsen, D. M. & Maricq, A. V. Action potentials contribute to neuronal signaling in C. elegans. *Nature Neuroscience* **11**, 865-867, doi:10.1038/nn.2131 (2008).

40 O'Hagan, R., Chalfie, M. & Goodman, M. B. The MEC-4 DEG/ENaC channel of Caenorhabditis elegans touch receptor neurons transduces mechanical signals. *Nat Neurosci* **8**, 43-50, doi:http://www.nature.com/neuro/journal/v8/n1/suppinfo/nn1362_S1.html (2005).

41 Larsch, J., Ventimiglia, D., Bargmann, C. I. & Albrecht, D. R. High-throughput imaging of neuronal activity in Caenorhabditis elegans. *Proceedings of the National Academy of Sciences of the United States of America* **110**, E4266-E4273, doi:10.1073/pnas.1318325110 (2013).

42 Suzuki, H. *et al.* Functional asymmetry in Caenorhabditis elegans taste neurons and its computational role in chemotaxis. *Nature* **454**, 114-117, doi:10.1038/nature06927 (2008).

43 Thiele, T. R., Faumont, S. & Lockery, S. R. The Neural Network for Chemotaxis to Tastants in Caenorhabditis elegans Is Specialized for Temporal Differentiation. *The Journal of Neuroscience* **29**, 11904-11911, doi:10.1523/jneurosci.0594-09.2009 (2009).

44 Liu, Q., Kidd, P. B., Dobosiewicz, M. & Bargmann, C. I. C. elegans AWA Olfactory Neurons Fire Calcium-Mediated All-or-None Action Potentials. *Cell* **175**, 57-70.e17, doi:https://doi.org/10.1016/j.cell.2018.08.018 (2018).

45 Pierce-Shimomura, J. T., Morse, T. M. & Lockery, S. R. The Fundamental Role of Pirouettes in Caenorhabditis elegans Chemotaxis. *The Journal of Neuroscience* **19**, 9557-9569, doi:10.1523/jneurosci.19-21-09557.1999 (1999).

46 Gourgou, E., Adiga, K., Goettemoeller, A., Chen, C. & Hsu, A.-L. Caenorhabditis elegans learning in a structured maze is a multisensory behavior. *iScience* **24**, 102284, doi:https://doi.org/10.1016/j.isci.2021.102284 (2021).

47 Marder, E. Neuromodulation of Neuronal Circuits: Back to the Future. *Neuron* **76**, 1-11, doi:https://doi.org/10.1016/j.neuron.2012.09.010 (2012).

48 Sulston, J., Dew, M. & Brenner, S. Dopaminergic neurons in the nematode Caenorhabditis elegans. *Journal of Comparative Neurology* **163**, 215-226, doi:10.1002/cne.901630207 (1975).

49 Sawin, E. R., Ranganathan, R. & Horvitz, H. R. C. elegans Locomotory Rate Is Modulated by the Environment through a Dopaminergic Pathway and by Experience through a Serotonergic Pathway. *Neuron* **26**, 619-631, doi:https://doi.org/10.1016/S0896-6273(00)81199-X (2000).

50 Hills, T., Brockie, P. J. & Maricq, A. V. Dopamine and glutamate control area-restricted search behavior in Caenorhabditis elegans. *J Neurosci* **24**, 1217-1225, doi:10.1523/jneurosci.1569-03.2004 (2004).

51 Chan, T. F. & Vese, L. A. Active contours without edges. *IEEE Transactions on Image Processing* **10**, 266-277, doi:10.1109/83.902291 (2001).

52 Gower, J. C. & Dijksterhuis, G. B. *Procrustes Problems*. Vol. 30 248 (Oxford University Press, 2004).

53 Nair, S. S., Paré, D. & Vicentic, A. Biologically based neural circuit modelling for the study of fear learning and extinction. *npj Science of Learning* **1**, 16015, doi:10.1038/npjscilearn.2016.15 (2016).

54 Iino, Y. & Yoshida, K. Parallel use of two behavioral mechanisms for chemotaxis in Caenorhabditis elegans. *The Journal of neuroscience : the official journal of the Society for Neuroscience* **29**, 5370-5380, doi:10.1523/JNEUROSCI.3633-08.2009 (2009).

55 Dusenbery, D. B. Analysis of chemotaxis in the nematode Caenorhabditis elegans by countercurrent separation. *The Journal of experimental zoology* **188**, 41-47, doi:10.1002/jez.1401880105 (1974).

56 Dusenbery, D. B. Responses of the nematodeCaenorhabditis elegans to controlled chemical stimulation. *Journal of comparative physiology* **136**, 327-331, doi:10.1007/bf00657352 (1980).

57 Schultz, W. Behavioral dopamine signals. *Trends Neurosci* **30**, 203-210, doi:10.1016/j.tins.2007.03.007 (2007).

58 Wise, R. A. Dopamine, learning and motivation. *Nat Rev Neurosci* **5**, 483-494, doi:10.1038/nrn1406 (2004).

59 Arias-Carrión, O., Stamelou, M., Murillo-Rodríguez, E., Menéndez-González, M. & Pöppel, E. Dopaminergic reward system: a short integrative review. *Int Arch Med* **3**, 24-24, doi:10.1186/1755-7682-3-24 (2010).

60 Wintle, R. F. & Van Tol, H. H. M. Dopamine signaling in Caenorhabditis elegans—potential for parkinsonism research. *Parkinsonism & Related Disorders* **7**, 177-183, doi:https://doi.org/10.1016/S1353-8020(00)00055-9 (2001).

61 Sanyal, S. *et al.* Dopamine modulates the plasticity of mechanosensory responses in Caenorhabditis elegans. *The EMBO Journal* **23**, 473-482, doi:10.1038/sj.emboj.7600057 (2004).

62 Kindt, K. S. *et al.* Dopamine mediates context-dependent modulation of sensory plasticity in C. elegans. *Neuron* **55**, 662-676, doi:10.1016/j.neuron.2007.07.023 (2007).

63 Qin, J. & Wheeler, A. R. Maze exploration and learning in C. elegans. *Lab Chip* **7**, 186-192, doi:10.1039/b613414a (2007).

64 Marder, E. Mechanisms underlying neurotransmitter modulation of a neuronal circuit. *Trends in Neurosciences* **7**, 48-53, doi:https://doi.org/10.1016/S0166-2236(84)80277-5 (1984).

65 Klingberg, T. Training and plasticity of working memory. *Trends in Cognitive Sciences* **14**, 317-324, doi:https://doi.org/10.1016/j.tics.2010.05.002 (2010).

66 Goldman-Rakic, P. S. Cellular basis of working memory. *Neuron* **14**, 477-485, doi:https://doi.org/10.1016/0896-6273(95)90304-6 (1995).

67 Compte, A., Brunel, N., Goldman-Rakic, P. S. & Wang, X.-J. Synaptic Mechanisms and Network Dynamics Underlying Spatial Working Memory in a Cortical Network Model. *Cerebral Cortex* **10**, 910-923, doi:10.1093/cercor/10.9.910 (2000).

68 Constantinidis, C. & Klingberg, T. The neuroscience of working memory capacity and training. *Nat Rev Neurosci* **17**, 438-449, doi:10.1038/nrn.2016.43 (2016).

69 Li, W., Feng, Z., Sternberg, P. W., Xu, X. Z. A C. elegans stretch receptor neuron revealed by a mechanosensitive TRP channel homologue. *Nature* **440**, 684-687, doi:10.1038/nature04538 (2006).

70 Han, B. *et al.* Dopamine signaling tunes spatial pattern selectivity in C. elegans. *eLife* **6**, e22896, doi:10.7554/eLife.22896 (2017).

71 Yeon, J. *et al.* A sensory-motor neuron type mediates proprioceptive coordination of steering in C. elegans via two TRPC channels. *PLOS Biology* **16**, e2004929, doi:10.1371/journal.pbio.2004929 (2018).

72 Kaplan, J. M. & Horvitz, H. R. A dual mechanosensory and chemosensory neuron in Caenorhabditis elegans. *Proc Natl Acad Sci U S A* **90**, 2227-2231, doi:10.1073/pnas.90.6.2227 (1993).

73 in *C. elegans II* (eds D. L. Riddle, T. Blumenthal, B. J. Meyer, & J. R. Priess) (Cold Spring Harbor Laboratory Press
Cold Spring Harbor Laboratory Press., 1997).

74 Kausler, B. *Learning and Memory in Normal Aging* (Academic Press, 1994).

75 Arey, R. N., Stein, G. M., Kaletsky, R., Kauffman, A. & Murphy, C. T. Activation of Gαq Signaling Enhances Memory Consolidation and Slows Cognitive Decline. *Neuron*, doi:https://doi.org/10.1016/j.neuron.2018.03.039 (2018).

76 Leung, N. T. *et al.* Neural Plastic Effects of Cognitive Training on Aging Brain. *Neural plasticity* **2015**, 535618, doi:10.1155/2015/535618 (2015).

77 Mattay, V. S. *et al.* Neurophysiological correlates of age-related changes in working memory capacity. *Neuroscience letters* **392**, 32-37, doi:https://doi.org/10.1016/j.neulet.2005.09.025 (2006).
78 Morcom, A. M. *et al.* Memory encoding and dopamine in the aging brain: a psychopharmacological neuroimaging study. *Cereb Cortex* **20**, 743-757, doi:10.1093/cercor/bhp139 (2010).
79 Backman, L., Nyberg, L., Lindenberger, U., Li, S. C. & Farde, L. The correlative triad among aging, dopamine, and cognition: current status and future prospects. *Neuroscience and biobehavioral reviews* **30**, 791-807, doi:10.1016/j.neubiorev.2006.06.005 (2006).
80 Leinwand, S. G. *et al.* Circuit mechanisms encoding odors and driving aging-associated behavioral declines in Caenorhabditis elegans. *Elife* **4**, e10181, doi:10.7554/eLife.10181 (2015).
81 Segovia, G., Porras, A., Del Arco, A. & Mora, F. Glutamatergic neurotransmission in aging: a critical perspective. *Mech Ageing Dev* **122**, 1-29, doi:10.1016/s0047-6374(00)00225-6 (2001).
82 Lippa, A. S. *et al.* Age-related alterations in neurotransmitter receptors: An electrophysiological and biochemical analysis. *Neurobiology of aging* **2**, 3-8, doi:https://doi.org/10.1016/0197-4580(81)90052-X (1981).
83 Cai, S. Q. & Sesti, F. Oxidation of a potassium channel causes progressive sensory function loss during aging. *Nat Neurosci* **12**, 611-617, doi:10.1038/nn.2291 (2009).
84 Branch, S. Y., Sharma, R. & Beckstead, M. J. Aging Decreases L-Type Calcium Channel Currents and Pacemaker Firing Fidelity in Substantia Nigra Dopamine Neurons. *The Journal of Neuroscience* **34**, 9310-9318, doi:10.1523/jneurosci.4228-13.2014 (2014).
85 Karbowski, J. Deciphering neural circuits for Caenorhabditis elegans behavior by computations and perturbations to genome and connectome. *Current Opinion in Systems Biology* **13**, 44-51, doi:https://doi.org/10.1016/j.coisb.2018.09.008 (2019).

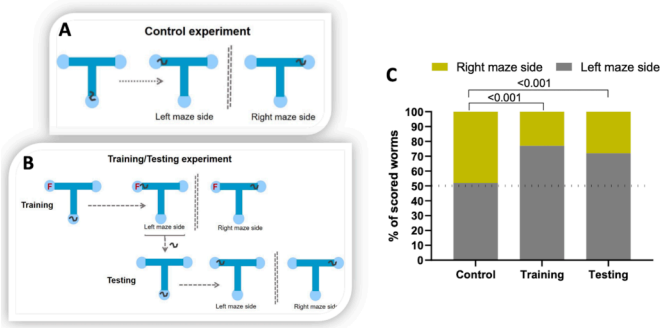

EJN_15560_Figure1.tiff

EJN_15560_Figure10.tiff

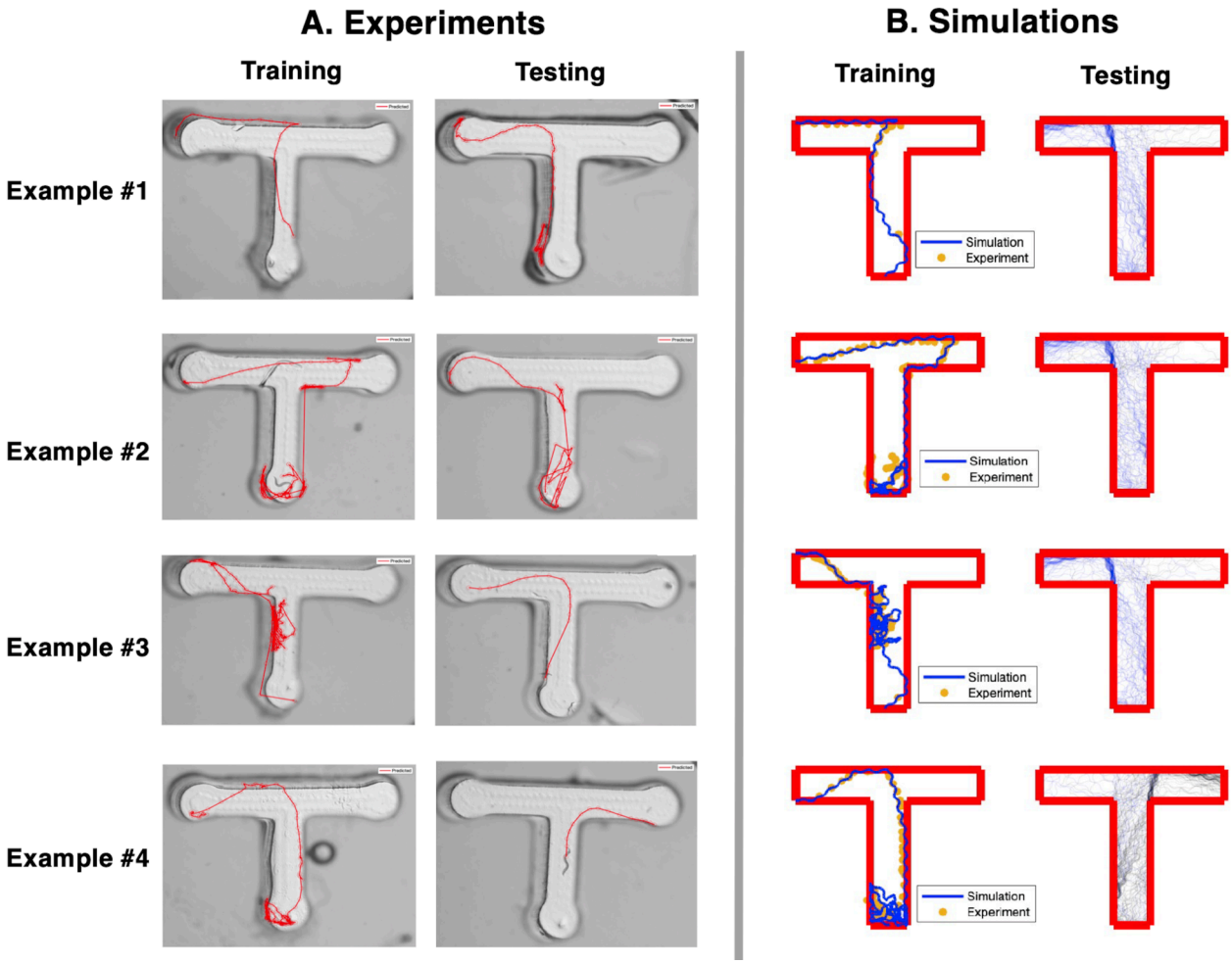

EJN_15560_Figure11.tiff

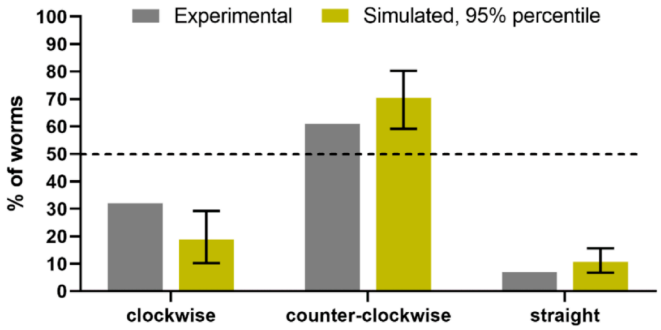

EJN_15560_Figure12.tiff

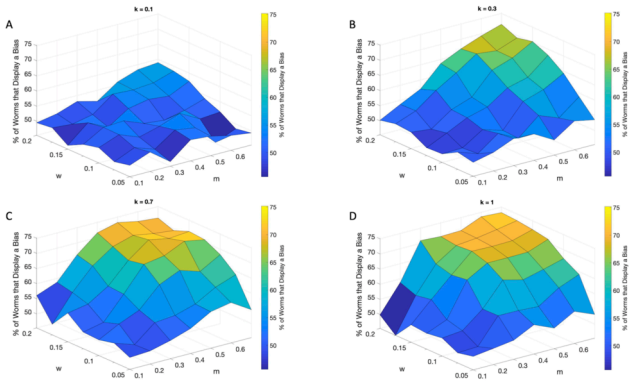

EJN_15560_Figure13.tiff